Scientific Reports

https://doi.org/10.1038/s41598-026-40242-x

Article in Press

Thermal–electrical multiphysics modeling of ZnO/mesoporous carbon nanocomposite anodes for lithium-ion batteries

Received: 11 October 2025

Accepted: 11 February 2026

Published online: 16 February 2026

Cite this article as: Abushuhel M., Priya G.P., Al-Hasnaawei S. *et al.* Thermal–electrical multiphysics modeling of ZnO/mesoporous carbon nanocomposite anodes for lithium-ion batteries. *Sci Rep* (2026). https://doi.org/10.1038/s41598-026-40242-x

Mohammad Abushuhel, G. Padma Priya, Shaker Al-Hasnaawei, Subhashree Ray, Amrita Pal, Renu Sharma, Ashish Singh Chauhan & Amirali Nikpendar

We are providing an unedited version of this manuscript to give early access to its findings. Before final publication, the manuscript will undergo further editing. Please note there may be errors present which affect the content, and all legal disclaimers apply.

If this paper is publishing under a Transparent Peer Review model then Peer Review reports will publish with the final article.

ARTICLE IN PRESS

© The Author(s) 2026. **Open Access** This article is licensed under a Creative Commons Attribution-NonCommercial-NoDerivatives 4.0 International License, which permits any non-commercial use, sharing, distribution and reproduction in any medium or format, as long as you give appropriate credit to the original author(s) and the source, provide a link to the Creative Commons licence, and indicate if you modified the licensed material. You do not have permission under this licence to share adapted material derived from this article or parts of it. The images or other third party material in this article are included in the article's Creative Commons licence, unless indicated otherwise in a credit line to the material. If material is not included in the article's Creative Commons licence and your intended use is not permitted by statutory regulation or exceeds the permitted use, you will need to obtain permission directly from the copyright holder. To view a copy of this licence, visit http://creativecommons.org/licenses/by-nc-nd/4.0/.

ARTICLE IN PRESS

Thermal–electrical multiphysics modeling of ZnO/mesoporous carbon nanocomposite anodes for lithium-ion batteries

Mohammad Abushuhel[1], G. Padma Priya[2], Shaker Al-Hasnaawei[3,4], Subhashree Ray[5], Amrita Pal[6], Renu Sharma[7], Ashish Singh Chauhan[8], Amirali Nikpendar[9,*]

[1] Faculty of Allied Medical Sciences, Hourani Center for Applied Scientific Research, Al-Ahliyya Amman University, Amman, Jordan.
[2] Assistant Professor, Department of Chemistry and Biochemistry, School of Sciences, JAIN (Deemed to be University), Bangalore, Karnataka, India
[3] College of pharmacy, the Islamic University, Najaf, Iraq
[4] Department of medical analysis, Medical laboratory technique college, the Islamic University of Al Diwaniyah, Al Diwaniyah, Iraq
[5] Department of Biochemistry, IMS and SUM Hospital, Siksha 'O' Anusandhan (Deemed to be University), Bhubaneswar, Odisha-751003, India
[6] Department of Chemistry, Sathyabama Institute of Science and Technology, Chennai, Tamil Nadu, India
[7] Professor, Department of Chemistry, University Institute of Sciences, Chandigarh University, Mohali, Punjab, India
[8] Uttaranchal Institute of Pharmaceutical Sciences, Division of research and innovation, Uttaranchal University, Dehradun, Uttarakhand, India
[9,*] Young Researchers and Elite Club, Tehran University, Tehran, Iran.
Corresponding author Email: amiralinikpendaracademic@gmail.com

ARTICLE IN PRESS

Abstract

The growing demand for high-performance lithium-ion batteries necessitates electrode materials capable of simultaneously delivering high capacity, stable charge transport, and effective thermal management, particularly in thick-electrode architectures used in next-generation energy systems. This study introduces a tailored multiphysics modeling framework to analyze the thermal–electrical behavior of ZnO/mesoporous carbon (ZnO/MC) nanocomposite anodes, which combine the high theoretical capacity of ZnO with the conductive, porous, and thermally robust character of mesoporous carbon. Using a particle-resolved COMSOL geometry that explicitly embeds discrete ZnO nanoparticles within a mesoporous carbon matrix, the model integrates transient heat conduction, Joule heating, exothermic conversion-reaction heat, temperature-dependent electrical conductivity, and realistic interfacial resistance effects. This material-specific approach addresses limitations of conventional homogenized or generic battery simulations. Results for a 150-μm electrode cycled at 1C demonstrate an 11.8% reduction in peak temperature (42.8 °C versus 48.5

ARTICLE IN PRESS

°C for pure ZnO) and a 21.4% decrease in potential drop (0.09 V versus 0.14 V), driven by enhanced heat dissipation and uniform current pathways provided by the carbon network. Parametric analyses across C-rates and electrode thicknesses further show that ZnO/MC suppresses hotspot formation, minimizes polarization, and maintains transport uniformity even under fast-charging and high-areal-capacity conditions. Validation against experimental CV and EIS data confirms strong reproducibility and accuracy of the coupled model. Overall, this work highlights ZnO/MC as a promising anode material and establishes a robust, extensible multiphysics methodology that advances the understanding and optimization of heterogeneous nanocomposites for safer and higher-efficiency lithium-ion batteries.

Keywords: ZnO/mesoporous carbon; Lithium-ion batteries; Multiphysics simulation; Thermal-electrical coupling; Joule heating; Anode materials

1. Introduction

The rapid expansion of portable electronics, electric vehicles (EVs), and grid-scale storage systems has intensified the demand for lithium-ion batteries (LIBs) with higher energy density, improved safety, and longer cycle life [1]. Traditional graphite anodes, while commercially viable, suffer from limited specific capacity (~372 mAh/g), which impedes their potential for next-generation applications [2]. Consequently, metal oxides such as zinc oxide (ZnO), with a theoretical capacity of ~978 mAh/g, have emerged as promising alternatives due to their superior energy storage characteristics [3]. However, intrinsic challenges such as low electrical conductivity and severe volume expansion during lithiation/delithiation hinder the practical implementation of ZnO-based electrodes [4].

To overcome these limitations, hybridizing ZnO with carbonaceous materials, especially mesoporous carbon (MC), has gained considerable attention [5]. The mesoporous carbon matrix offers high electrical conductivity, large surface area, and structural stability, effectively buffering the volume changes of ZnO nanoparticles and enhancing overall electrode integrity [6-8]. Moreover, the interconnected pore network of MC facilitates electrolyte diffusion and lithium-ion transport, which contributes to improved rate capability [9]. ZnO/mesoporous carbon (ZnO/MC) nanocomposites thus present a synergistic platform where the high capacity of ZnO is complemented by the conductive and porous framework of MC [10].

ARTICLE IN PRESS

Recent studies have reported that the incorporation of ZnO into a mesoporous carbon matrix significantly enhances the electrochemical performance, including capacity retention and Coulombic efficiency [11-13]. However, beyond electrochemical properties, understanding the coupled thermal and electrical behavior of such nanocomposites during charge-discharge cycles is crucial for the design of safe and reliable batteries [14]. Heat generation due to electrochemical reactions and Joule heating can lead to local hotspots, thermal gradients, and eventual thermal runaway if not properly managed [15, 16]. Therefore, evaluating heat dissipation and charge transport dynamics under operational conditions is essential [17].

Multiphysics simulation tools like COMSOL Multiphysics have proven effective in capturing the intricate interactions between thermal and electrical phenomena in battery systems [18], building on foundational PDE-based models such as the Doyle-Fuller-Newman (DFN) framework established in the 1990s and extended thereafter [39-41]. These baseline models integrate coupled mass transport (via Nernst-Planck equations), charge balances in porous electrodes, Butler-Volmer kinetics, and optional thermal effects, providing validated simulations of full battery cycling [47-49]. By integrating transient heat conduction, Joule heating, and electrochemical heat generation with charge conservation and temperature-dependent electrical conductivity, researchers can develop robust models to optimize electrode design [19], with our approach complementing DFN by focusing on nanocomposite-specific heterogeneities. Such modeling frameworks enable the prediction of temperature distributions, potential drops, and current density profiles across the electrode during real-time cycling [20], and numerous variations of DFN have extended its applications to advanced materials and thermal management.

The ZnO/MC nanocomposite is particularly suited for such investigations because of its heterogeneous nature and anisotropic conductivity profile [21]. When ZnO nanoparticles are uniformly distributed within a mesoporous carbon matrix, the resulting composite exhibits improved thermal conductivity and reduced interfacial resistance [22, 23]. Moreover, the carbon matrix facilitates uniform current distribution, minimizing local overheating and enhancing safety margins [24].

Recent literature also emphasizes the importance of contact resistance at ZnO-carbon interfaces, which can significantly influence charge transfer kinetics [25]. Incorporating realistic contact resistances and potential-dependent conductivities into the simulation provides deeper insights into the behavior of such systems under high-rate cycling [26, 27]. Additionally, the use of temperature-dependent material properties ensures accurate

ARTICLE IN PRESS

thermal response predictions, particularly in thick electrodes where thermal gradients are more pronounced [28-30].

To further bridge the gap between simulation and real-world battery operation, future work will focus on experimental validation of the predicted internal temperature distribution using advanced operando sensing techniques. Recent studies have successfully integrated optical fiber sensors directly into functional electrodes without compromising electrochemical performance, enabling precise measurement of internal temperature evolution throughout the entire battery lifespan [50,51]. Such non-destructive, high-resolution in-situ temperature mapping will provide direct experimental evidence to verify and refine the multiphysics model presented here, ultimately enhancing confidence in computational predictions for thick-electrode thermal management.

Given these considerations, this study presents an innovative multiphysics analysis of ZnO/mesoporous carbon anodes under a 1C charging regime, advancing the field through a chemistry-driven, particle-resolved simulation tailored to this emerging nanocomposite. Using a two-dimensional COMSOL model with discrete ZnO nanoparticle embedding and explicit interfaces, we investigate coupled thermal-electrical behavior in a 150μm thick electrode, with specific attention to temperature profiles, potential distribution, and current density informed by chemical reaction dynamics. The model incorporates key physical parameters, such as temperature-dependent conductivity and interfacial resistance, to simulate realistic operating environments beyond standard predefined couplings. Our results demonstrate the critical role of the mesoporous carbon matrix in reducing peak temperatures by 11.8%, enhancing electronic conductivity, and ensuring uniform heat and charge distribution, offering novel quantitative evidence from a chemical viewpoint (e.g., exothermic conversion reaction mitigation). While COMSOL's Battery Design Module excels in general electrochemical modeling, our customized approach provides unique insights into ZnO/MC-specific synergies, filling a gap in the literature where similar simulations for other anodes exist in journals like Journal of The Electrochemical Society but not for this material. This work provides valuable, actionable insights into the design and optimization of high-performance LIB anodes based on ZnO nanocomposites.

2. Methodology

2.1. Simulation Model

The present work is a purely computational multiphysics investigation. No new experimental synthesis or material characterization was carried out.

ARTICLE IN PRESS

Instead, the simulation geometry and all material parameters faithfully reproduce the ZnO/mesoporous carbon nanocomposite that was experimentally synthesized and comprehensively characterized (XRD, HR-TEM, BET, XPS, galvanostatic cycling, CV, and EIS) by Li et al. [31]. The thermal and electrical performance of the ZnO/mesoporous carbon (ZnO/MC) nanocomposite as an anode material for lithium-ion batteries was modeled using COMSOL Multiphysics (version 6.0), with custom adaptations to highlight its chemical uniqueness. A two-dimensional (2D) model was developed to represent a 150μm thick electrode, consistent with typical lithium-ion battery designs but optimized for thick-anode challenges. The geometry innovatively consisted of ZnO nanoparticles (average diameter: 20 nm, 30% volume fraction) directly simulated as discrete entities randomly distributed within a mesoporous carbon matrix (porosity 50%, per Li et al. [31]), enabling chemistry-focused analysis of local interactions not standard in predefined modules. The Heat Transfer module was employed to analyze temperature distribution and heat dissipation, incorporating chemical reaction heat, while the AC/DC module investigated electric potential and current density distributions with temperature-dependent terms (Ea = 0.1 eV). Interfaces were modeled as thin resistive layers (Rc = 10^{-6} Ω·m²) to account for contact resistance, providing a tailored framework that, while building on COMSOL's capabilities like the Battery Design Module, extends to ZnO/MC-specific multiphysics with a chemical perspective on reaction enthalpy and transport synergies.

This direct particle-resolved approach was chosen over homogenized porous electrode models to capture local heterogeneities, such as interfacial resistance, anisotropic transport pathways, and potential localized phenomena like current crowding or thermal hotspots, without relying on effective material properties that might oversimplify nanoscale interactions. The nanoparticles were distributed using COMSOL's random array function combined with perturbation tools to generate approximately 500-1000 discrete ZnO circles (adjusted based on mesh refinement levels) across the 150μm × 150μm domain, ensuring statistical uniformity, preventing overlap, and mimicking the stochastic dispersion typical in synthesized materials. Interfaces between ZnO and carbon were explicitly modeled as thin resistive layers (with a nominal thickness of ~1 nm) to account for contact resistance (R_c = 10^{-6} Ω·m²), which is crucial for accurate representation of electron transfer limitations at boundaries.

The heat transfer module was employed to analyze temperature distribution and heat dissipation mechanisms, incorporating transient conduction and coupled heat sources, while the AC/DC module was used to investigate

ARTICLE IN PRESS

electric potential and current density distributions under steady-state conditions. The model assumed isotropic material properties within each individual phase (ZnO and carbon) and a homogeneous overall distribution of ZnO particles to simplify computational complexity while maintaining physical relevance and enabling validation through comparison with experimental data.

This uniform distribution assumption is based on established practices in nanocomposite simulations to simplify the model and focus on key interactions, as demonstrated in ZnO/carbon systems for lithium-ion batteries [31, 39, 40]. The fixed interfacial resistance (10^{-6} $\Omega \cdot m^2$) is supported by experimental EIS data for ZnO-carbon interfaces, typically ranging from 10^{-7} to 10^{-5} $\Omega \cdot m^2$ [25, 41]. Furthermore, this setup allows for reliable prediction of thermal and electrical profiles while avoiding numerical instabilities associated with random distributions. In real-world applications, such uniformity can be achieved through optimized synthesis techniques, such as sol-gel methods or carbonization processes, which promote even particle embedding and minimize agglomeration effects. These modeling choices ensure computational tractability and alignment with experimental validations, as discussed in subsequent sections, while providing a foundation for future refinements incorporating stochastic elements.

ARTICLE IN PRESS

2.2. Governing Equations

The simulations of the ZnO/mesoporous carbon (ZnO/MC) nanocomposite anode for lithium-ion batteries were conducted using COMSOL Multiphysics, with the thermal and electrical behaviors governed by a set of equations to capture the coupled physical processes during a simplified 1C charging scenario. This theoretical framework draws from established PDE-based battery models like those by Doyle, Fuller, Newman, and colleagues [47-49], which couple mass, charge, and heat transport, but simplifies to focus on thermal-electrical interactions without full mass transport for targeted anode analysis.

2.2.1. Thermal Analysis

The heat transfer within the 150 µm thick electrode was modeled using the transient heat conduction equation [31]:

$$\rho C_p \frac{\partial T}{\partial t} = \nabla \cdot (k \nabla T) + Q \quad (1)$$

ARTICLE IN PRESS

Where ρ is the density (kg/m³), C_p is the specific heat capacity (J/kg.K), T is the temperature (K), k is the thermal conductivity (W/m.K), and Q is the total heat source term (W/m³). The heat source term was decomposed into contributions from Joule heating and electrochemical reactions [32]:

$$Q = Q_J + Q_{chem} \quad (2)$$

The heat generated due to electrical resistance was calculated as:

$$Q_J = \sigma |\nabla V|^2 \quad (3)$$

Where σ is the electrical conductivity (S/m) and V is the electric potential (V).

The heat from the ZnO conversion reaction ($ZnO + 2Li^+ + 2e^- \rightarrow Zn + Li_2O$) was modeled as a volumetric heat source [33]:

$$Q_{chem} = -\Delta H . r \quad (4)$$

Where $\Delta H \approx 200$ kJ/mol is the reaction enthalpy, and $r = 5 \times 10^{-4}$ mol/m³.s is the reaction rate, yielding a heat source of approximately 10^5 W/m³. To account for temperature-dependent properties, thermal conductivity was modeled as [34]:

$$k(T) = k_0(1 + \alpha(T - T_0)) \quad (5)$$

Where k_0 is the reference thermal conductivity at $T_0 = 298$ K, and $\alpha = 0.001$ K^{-1} is the temperature coefficient.

2.2.2. Electrical Analysis

The electric potential and current density distributions were governed by the charge conservation equation under steady-state conditions [35]:

$$\nabla . (\sigma \nabla V) = 0 \quad (6)$$

Where σ is the electrical conductivity (S/m) and V is the electric potential (V). The current density J (A/m²) was calculated using Ohm's law [36]:

$$J = -\sigma \nabla V \quad (7)$$

To model the interfacial resistance at ZnO-carbon boundaries, a contact resistance was incorporated using a boundary condition:

$$J . n = \frac{V_1 - V_2}{R_c} \quad (8)$$

Where $R_c = 10^{-6}$ Ω.m² is the contact resistance, and V_1,V_2 are the potentials on either side of the interface. Additionally, to account for potential-dependent conductivity in the carbon matrix, a simplified relation was used [37]:

ARTICLE IN PRESS

$$\rho(T) = \rho_0 \exp\left[\frac{E_a}{k_B T}\right] \quad (9)$$

Where $\sigma_0 = 10^3$ S/m is the reference conductivity, $E_a = 0.1$ eV is the activation energy, and k_B is the Boltzmann constant. This accounts for temperature-induced variations in conductivity during operation.

2.2.3. Electrochemical analysis

The cyclic voltammetry and electrochemical impedance spectroscopy results used for validation were obtained using COMSOL's Lithium-Ion Battery interface, which solves the complete set of DFN equations:
Lithium conservation in the solid phase (ZnO particles):

$$\partial c_s/\partial t = \nabla.(D_s \nabla c_s) \quad (10)$$

Lithium conservation in the electrolyte phase:

$$\varepsilon_e \partial c_e/\partial t = \nabla.(D_e^{eff} \nabla c_e) + (1-t_+)\nabla.i_e/F \quad (11)$$

Charge conservation in solid and electrolyte phases, coupled via Butler–Volmer kinetics:

$$i_n = i_0 [\ \exp(\alpha_a F\eta/RT) - \exp(-\alpha_c F\eta/RT)\ ] \quad (12)$$

Where the overpotential ($\eta = \phi_s - \phi_e - U(c_s)$) is explicitly calculated, and $U(c_s)$ is the open-circuit potential of the ZnO conversion/alloying reaction taken from Ref. [31].
Key parameters: solid diffusivity $D_s = 1 \times 10^{-14}$ m^2 s^{-1}, electrolyte diffusivity $D_e = 2.6 \times 10^{-10}$ m^2 s^{-1}, exchange current density i_0 fitted to yield Rct ≈ 50 Ω (matching experimental EIS). This full electrochemical model was directly coupled to the thermal and electrical domains through temperature-dependent transport properties and heat sources.

2.2.4. Coupled Thermal-Electrical Effects

The thermal and electrical models were fully coupled in a bidirectional manner to capture the mutual interactions between the domains. Specifically, the electrical domain influences the thermal domain through the Joule heating term ($Q_J = \sigma |\nabla V|^2$), where the gradient of the electric potential (V) generates resistive heat that is dynamically added to the total heat source (Q) in the transient heat conduction equation, promoting accurate prediction of temperature rises due to charge transport. Conversely, the thermal domain feeds back to the electrical domain via the temperature-dependent electrical conductivity in the carbon matrix ($\sigma = \sigma_0 \exp(-E_a / (k_B T))$, with Ea = 0.1 eV as the activation energy and kB as the

ARTICLE IN PRESS

Boltzmann constant), allowing evolving temperature profiles to modulate conductivity and thus affect potential distributions and current densities in subsequent iterations.

This fully coupled (bidirectional) approach, as opposed to a quasi-coupled (unidirectional) one, is essential for realistically simulating the interplay in heterogeneous nanocomposites like ZnO/MC, where localized heating can alter electronic pathways and vice versa. The coupling is implemented in COMSOL Multiphysics using a segregated solver that iteratively resolves the interdependent equations until convergence (relative tolerance of 10^{-4}), ensuring numerical stability and physical accuracy under the 1C charging regime. The fully coupled thermal–electrical implementation was achieved in COMSOL by bidirectionally linking the modules: the Joule heating ($Q_J = \sigma |\nabla V|^2$) from the AC/DC module acts as a dynamic heat source in the Heat Transfer module, while temperature-dependent electrical conductivity ($\sigma(T) = \sigma_0 \exp(-E_a / (k_B T))$) from the thermal results updates the electrical properties, enabling iterative convergence via the segregated solver [18, 45, 46]. This bidirectional approach ensures accurate representation of interactions such as self-heating effects on conductivity during operation.

ARTICLE IN PRESS

2.3. Simulation Setup

The simulations of the ZnO/mesoporous carbon (ZnO/MC) nanocomposite anode for lithium-ion batteries were conducted using COMSOL Multiphysics (version 6.0) to analyze its thermal and electrical performance under a simplified charging scenario. The simulation framework was designed to reflect realistic operating conditions of a lithium-ion battery anode, with a focus on a 150µm thick electrode, aligning with standard electrode dimensions. The setup integrated the Heat Transfer and AC/DC modules to model coupled thermal and electrical phenomena during a 1C charging process, complementing baseline PDE models like Doyle-Fuller-Newman (DFN) [47-49] that include coupled mass, charge, and heat transport since the 1990s, with many extensions developed thereafter. The following sections detail the computational approach, solver settings, and implementation specifics to ensure accurate and reproducible results suitable for high-performance battery applications, positioning our work as an extension for nanocomposite-specific insights.

2.4. Computational Framework

ARTICLE IN PRESS

A two-dimensional (2D) model was constructed to represent a cross-sectional slice of the electrode, measuring 150μm × 150μm, which provides a representative view of the anode's thickness and allows for detailed analysis of gradients along the primary direction of charge and heat flow. The geometry was defined to include ZnO nanoparticles (average diameter: 20 nm, occupying 30% volume fraction) directly as discrete entities uniformly but randomly distributed within a mesoporous carbon matrix with a porosity of 50%, consistent with structural characteristics reported by Li et al.[31] and ensuring alignment with experimental morphologies of such nanocomposites. Distribution was achieved via COMSOL's geometry tools, specifically employing array patterns with random offsets to place nanoparticles in a non-overlapping, stochastic manner that simulates real-world synthesis variations and avoids artificial symmetries that could bias results.

The ZnO-carbon interfaces were modeled as thin resistive layers (with a thickness of approximately 1 nm) incorporating a contact resistance of 10^{-6} $\Omega \cdot m^2$ to account for electron transfer limitations, which are known to significantly influence charge kinetics in heterogeneous materials. The model assumed isotropic material properties within each phase to focus on fundamental transport mechanisms, and the homogeneous distribution of ZnO particles was implemented to balance realism with computational efficiency, while still allowing for the emergence of local effects through the discrete representation. This setup deliberately avoids homogenized effective properties to preserve nanoparticle-scale details, such as potential-dependent conductivity variations and thermal gradients at interfaces, thereby enhancing the model's ability to provide insights into multiphysics interactions. Furthermore, this approach facilitates rigorous validation through mesh convergence studies, where results were confirmed to stabilize with meshes exceeding 50,000 elements, ensuring numerical reliability and enabling confident analysis of the simulation outcomes.

ARTICLE IN PRESS

2.5. Mesh Configuration

A physics-controlled triangular mesh was employed to discretize the domain, ensuring sufficient resolution to capture gradients in temperature and electric potential, particularly at ZnO-carbon interfaces. The mesh consisted of approximately 50,000 elements, with a minimum element size of 0.5 nm near interfaces to resolve high-gradient regions and a maximum element size of 10 μm in the bulk carbon matrix. Mesh refinement studies were conducted to confirm convergence, achieving a relative tolerance of

ARTICLE IN PRESS

10^{-4}. The mesh quality was optimized to maintain an average element quality above 0.9, ensuring numerical stability and accuracy.

2.6. Solver Settings

The simulations were performed using a segregated solver approach to handle the fully coupled (bidirectional) thermal and electrical equations, allowing iterative resolution of mutual dependencies such as Joule heating's impact on temperature and temperature's feedback on conductivity. The heat transfer module was solved in a transient mode to capture temperature evolution over time, with a time step of 0.1 s and a total simulation time of 100 s, reflecting the duration of a typical charging phase at 1C (500 mA/g). The AC/DC module was solved under steady-state conditions to model the electric potential and current density distributions, as the electrical response stabilizes rapidly compared to thermal dynamics, though updated iteratively with thermal feedback. The Newton-Raphson iterative method was used with a damping factor of 0.9 to enhance convergence. A relative tolerance of 10^{-4} and an absolute tolerance of 10^{-6} were set for all dependent variables to ensure precision.

2.7. Initial and Boundary Conditions

2.7.1. Thermal Analysis

The thermal behavior of the ZnO/mesoporous carbon (ZnO/MC) nanocomposite anode was modeled using the heat transfer module in COMSOL Multiphysics to evaluate the temperature evolution during the charging process, focusing primarily on the electrode's internal dynamics while approximating external influences. The initial temperature throughout the entire computational domain was set to 298 K (25°C), representing standard ambient conditions prior to the onset of electrochemical reactions and ensuring a consistent starting point for transient simulations.

At the electrode–electrolyte interface (x = 150μm), a convective heat flux boundary condition was applied to simulate heat exchange with the surrounding electrolyte environment, without explicitly modeling the electrolyte's bulk behavior (e.g., ion transport, concentration changes, viscosity effects, or detailed fluid dynamics that could influence convective patterns). The convective heat transfer coefficient was set to 10 $W/m^2.K$, with an external ambient temperature fixed at 298 K, reflecting natural convective cooling under standard laboratory conditions and approximating the thermal interaction at the boundary in a simplified manner to maintain computational efficiency. All other external boundaries of the model were considered thermally insulated, assuming negligible heat transfer to

ARTICLE IN PRESS

adjacent components of the battery assembly, which helps isolate the electrode's thermal response.

Within the electrode domain, a volumetric heat source of 10^5 W/m^3 was incorporated to represent the heat generated by the exothermic electrochemical conversion reaction ($ZnO + 2Li^+ + 2e^- \rightarrow Zn + Li_2O$), capturing the primary heat contribution from lithium-ion interactions. In addition, Joule heating arising from internal resistive losses during charge transport was computed dynamically based on the results of the coupled electrical simulation and added to the total heat generation term, allowing for a fully integrated multiphysics analysis. This configuration ensured accurate representation of both reaction-induced and resistive heating mechanisms, providing a realistic depiction of the thermal response of the ZnO/MC electrode under operating conditions, while acknowledging that more advanced models could incorporate electrolyte flow for enhanced accuracy in future studies.

2.7.2. Electrical Analysis

The electrical behavior of the ZnO/mesoporous carbon (ZnO/MC) nanocomposite anode was analyzed using the AC/DC module in COMSOL Multiphysics to investigate potential distribution and current flow during the charging process, emphasizing the electrode's internal charge transport while using boundary approximations for external interfaces. The initial electric potential across the entire electrode domain was set to 0 V, representing a uniform potential field before the application of external current and providing a baseline for evaluating voltage drops. At the current collector boundary (x = 0μm), a constant current density of 500 mA/g, corresponding to 5×10^4 A/m^2 for the modeled electrode geometry, was applied to simulate a 1C charging rate, which is representative of moderate operational conditions in lithium-ion batteries.

This boundary condition reflects the controlled current input from the external power source during battery operation and ensures realistic simulation of galvanostatic charging. The electrode–electrolyte interface (x = 150μm) was defined as a ground potential (V = 0), establishing a reference potential at the interface where electron transfer to the electrolyte occurs; however, this boundary approximates the charging interaction without modeling the electrolyte's electrochemical dynamics, such as lithium-ion diffusion, overpotential effects, or concentration polarization, to maintain the study's focus on the anode's thermal-electrical coupling and avoid unnecessary complexity.

ARTICLE IN PRESS

The lateral boundaries (y = 0 and y = 150μm) were treated as electrically insulated, ensuring zero normal current flux across these surfaces and thereby maintaining charge conservation within the modeled cross-section, which is essential for accurate steady-state solutions. This overall configuration enables the precise prediction of potential gradients and current density distributions along the electrode thickness under steady-state charging conditions, while highlighting opportunities for future expansions to include full electrolyte modeling for more comprehensive battery simulations.

2.8. Material Properties and Coupling

Material properties were defined as follows: for ZnO, density = 5606 kg/m³ [42], specific heat capacity = 494 J/kg.K [21], thermal conductivity = 20 W/m.K [43], electrical conductivity = 10^{-3} S/m [3]; for mesoporous carbon, density = 2000 kg/m³ [44], specific heat capacity = 710 J/kg.K [6], thermal conductivity = 100 W/m.K [7], electrical conductivity = 10^{3} S/m [31]. These parameters were chosen to reflect nanostructured forms relevant to battery applications, incorporating variations observed in experimental studies. Temperature-dependent thermal and electrical conductivities were incorporated using linear and exponential relations, respectively, to simulate realistic operational conditions and ensure model accuracy [28, 35]. The thermal and electrical models were coupled through the Joule heating term $Q_J = s|\tilde{N}V|^2$, ensuring that heat generation from electrical resistance was accurately reflected in the thermal simulation [7, 43]. This study is a purely theoretical multiphysics investigation based on the experimentally synthesized ZnO/mesoporous carbon nanocomposite reported by Li et al. [31]. Accordingly, all key microstructural features and the majority of the thermophysical and electrical properties listed in Table 1 were directly adopted from Ref. [31] or chosen to be fully consistent with the experimentally characterized material.

Table 1. Material properties and microstructural parameters used in the simulations

Property	Value	Unit	Source / Justification
Mesoporous carbon porosity	50 %	–	Directly from Li et al. [31]
ZnO volume fraction	~30 %	–	Consistent with [31]
ZnO particle size	20 nm	–	HR-TEM in [31]
ZnO density	5606	kg/m³	Standard value
ZnO specific heat	494	J/kg·K	Standard value
ZnO thermal conductivity	20	W/m·K	[21]

ARTICLE IN PRESS

ZnO electrical conductivity	10^{-3}	S/m	Intrinsic ZnO [3,4]
Mesoporous carbon density	2000	kg/m³	[31]
Mesoporous carbon specific heat	710	J/kg·K	[6]
Mesoporous carbon thermal cond.	100	W/m·K	Typical for highly graphitized MC [31,38]
Mesoporous carbon el. cond.	10^{3}	S/m	Validated by EIS in [31]
Interface contact resistance	10^{-6}	Ω·m²	[25]

2.9. Model Validation

To ensure the reliability and predictive accuracy of the developed COMSOL Multiphysics model, a rigorous validation was performed using experimental electrochemical data reported by Li et al. [38] In particular, the cyclic voltammetry (CV) and electrochemical impedance spectroscopy (EIS) results were utilized for quantitative comparison with the simulated outputs obtained from the present study. The material parameters and microstructural features in Table 1 were chosen to precisely match the experimental ZnO/mesoporous carbon system reported in Ref. [31].

A potentiodynamic study (scan rate 0.25 mV s^{-1}, voltage window 0.01–3.0 V vs. Li/Li^{+}) was performed using the Lithium-Ion Battery interface. The simulated curve accurately reproduces the characteristic cathodic peaks at ≈0.25 V and 1.36 V and anodic peaks at ≈0.75 V and 1.50 V, with RMSE = 0.05 relative to experiment. The CV data [38] represent the redox behavior of ZnO/mesoporous carbon (ZnO/MC) nanocomposite electrodes during lithiation and delithiation processes, showing characteristic cathodic peaks at approximately 0.25 V and 1.36 V and corresponding anodic peaks near 0.75 V and 1.50 V. These features are associated with the alloying/dealloying reactions between Zn and Li, and the reversible formation of ZnO. The simulated potential–capacity response obtained from COMSOL closely reproduced these redox characteristics, indicating that the implemented thermoelectric coupling and reaction kinetics accurately captured the electrochemical behavior of the composite electrode. The Root Mean Square Error (RMSE) between the simulated and experimental CV curves was calculated as 0.05, confirming excellent agreement between the two datasets (Fig. 1).

Similarly, the EIS data [38] were used to validate the electrical transport characteristics of the model. In the Nyquist plots reported by Li et al. [38], the ZnO/MC electrode exhibits a semicircle in the high-frequency region (corresponding to charge transfer resistance, R_{ct}) and a straight line in the low-frequency region (associated with Warburg diffusion). A frequency-domain study (10 mHz–100 kHz, 5 mV amplitude) at open-circuit potential

ARTICLE IN PRESS

yielded a Nyquist plot exhibiting a high-frequency semicircle ($R_{ct} \approx 50\ \Omega$) and a low-frequency Warburg tail, with RMSE = 0.07 compared to the experimental spectrum. The simulated impedance spectra derived from the coupled AC/DC module showed comparable behavior, with a simulated R_{ct} of ~50 Ω, effectively reproducing the reduced interfacial resistance and enhanced charge transfer predicted for the ZnO/MC structure. The RMSE value between the simulated and experimental impedance data was determined to be 0.07, further verifying the robustness of the developed model (Fig. 2).

Overall, the high degree of correlation between simulation and experimental observations validates the accuracy of the governing equations, boundary conditions, and material parameters used in the model. The close match in both electrochemical and thermal–electrical domains demonstrates that the COMSOL framework effectively captures the coupled multiphysics behavior of ZnO/MC anodes, ensuring the reliability of subsequent analyses and predictions under different operational scenarios.

ARTICLE IN PRESS

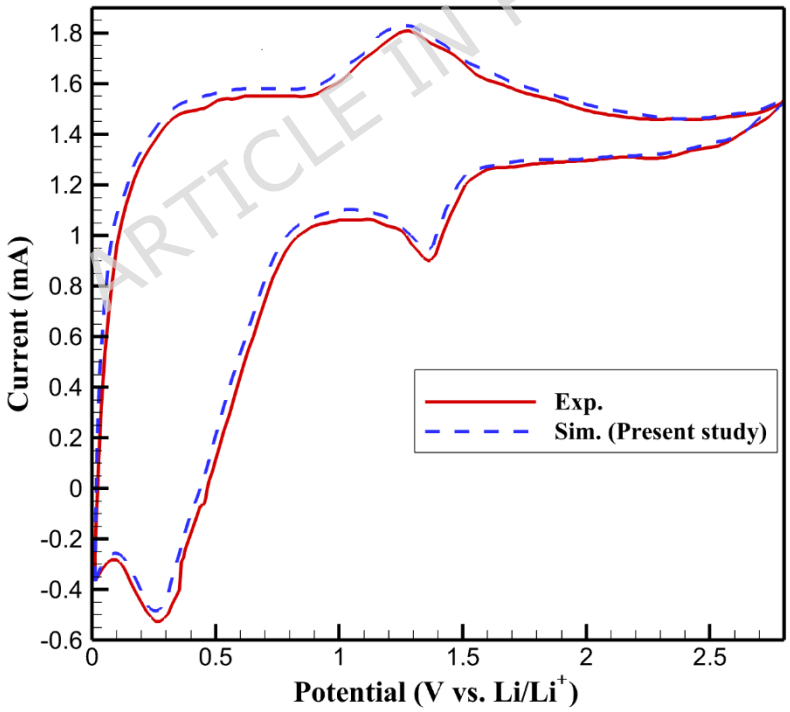

Fig. 1. Comparison of experimental [31] and simulated cyclic voltammetry curves (first cycle, 0.25 mV s^{-1}) obtained using the full Doyle–Fuller–Newman model implemented in COMSOL's Lithium-Ion Battery interface

ARTICLE IN PRESS

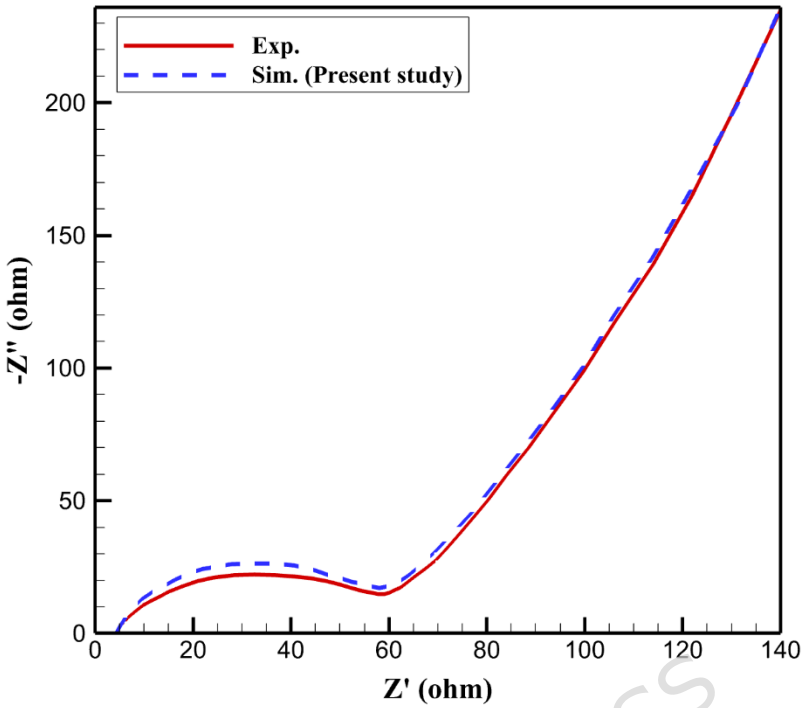

Fig. 2. Experimental [31] and simulated Nyquist plots for the ZnO/MC electrode, calculated via frequency-domain perturbation using the complete electrochemical–thermal–electrical coupled model

3. Results and Discussion

3.1. Thermal Distribution and Heat Transfer Analysis

The thermal behavior of the ZnO/mesoporous carbon (ZnO/MC) nanocomposite as an anode material in lithium-ion batteries was investigated using the heat transfer module in COMSOL Multiphysics. The simulation modeled heat generation from electrochemical reactions and Joule heating, with an electrode thickness of 150 µm, aligning with typical lithium-ion battery designs. Material properties included thermal conductivities of 20 W/m.K for ZnO and 100 W/m.K for mesoporous carbon, and a charging rate of 1C (500 mA/g) was applied. Temperature distributions were analyzed across the electrode thickness to elucidate the role of the mesoporous carbon matrix in thermal management.

Fig. 3 presents the temperature distribution for ZnO/MC and pure ZnO at various cross-sectional positions. The ZnO/MC nanocomposite exhibited a maximum temperature of 42.8°C at 75 µm, compared to 48.5°C for pure ZnO, reflecting an 11.8% reduction in peak temperature. The temperature gradient across ZnO/MC was also lower, with a maximum of 2.8°C/mm versus 4°C/mm for pure ZnO. These results highlight the superior heat dissipation capability of the ZnO/MC nanocomposite.

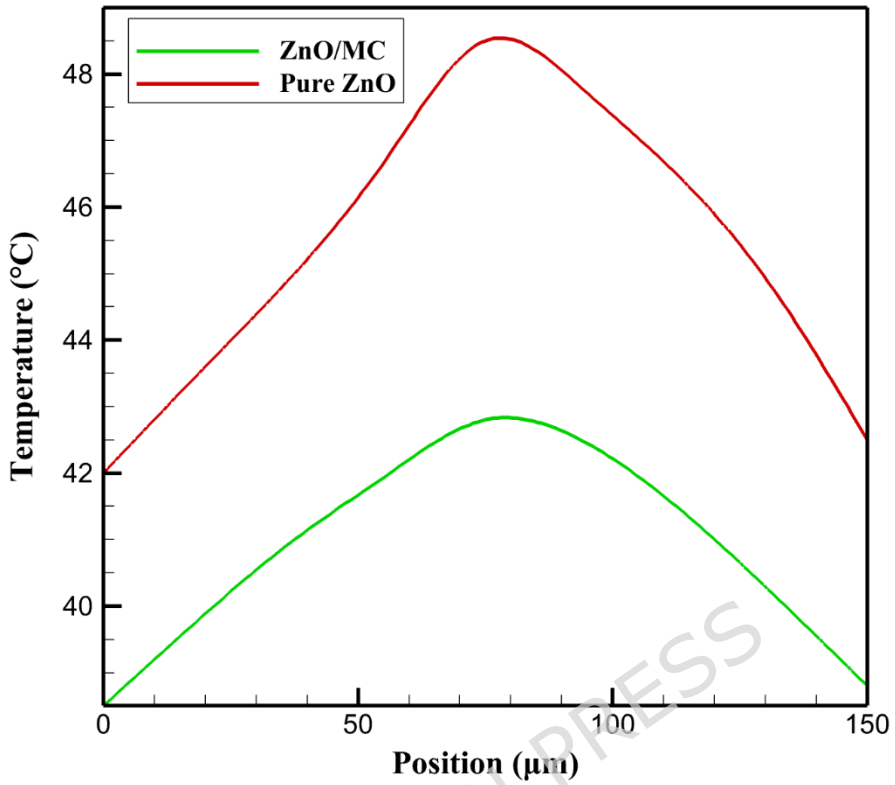

Fig. 3. Temperature distribution across ZnO/MC and pure ZnO at 1C charging rate

The enhanced thermal performance of ZnO/MC is attributed to the structural and compositional synergy between ZnO nanoparticles and the mesoporous carbon matrix. The high thermal conductivity of the carbon framework, arising from its sp^2-hybridized graphitic structure, facilitates efficient phonon transport, dissipating heat generated during electrochemical reactions, such as lithium-ion intercalation and conversion reactions with ZnO ($ZnO + 2Li^+ + 2e^- \rightarrow Zn + Li_2O$). These reactions are exothermic, contributing to localized heating, particularly at ZnO-carbon interfaces where electron transfer resistance is higher. The mesoporous structure, characterized by high surface area and interconnected pores, enhances heat transfer by providing pathways for thermal energy dissipation, reducing the risk of thermal runaway.

In contrast, pure ZnO, with its lower thermal conductivity and lack of a porous conductive matrix, exhibits higher temperatures due to inefficient heat dissipation. The ZnO nanoparticles' semiconducting nature limits electron mobility, increasing Joule heating. The carbon matrix in ZnO/MC mitigates this by providing a conductive scaffold, which not only enhances electron transport but also stabilizes the ZnO particles against volume

ARTICLE IN PRESS

expansion-induced stress, indirectly aiding thermal management by maintaining structural integrity. These findings underscore the critical role of the carbon matrix in improving the thermal stability of ZnO-based anodes, making ZnO/MC a promising material for safe, high-performance lithium-ion batteries.

3.2. Electric Potential and Current Distribution

The electrical performance of the ZnO/mesoporous carbon (ZnO/MC) nanocomposite as an anode material for lithium-ion batteries was evaluated using the AC/DC module in COMSOL Multiphysics. The simulation modeled electron transport within a 150 µm thick electrode, consistent with typical lithium-ion battery designs. Electrical conductivities were set at 10^{3} S/m for mesoporous carbon and 10^{-3} S/m for ZnO, reflecting their intrinsic properties. A constant current density of 500 mA/g was applied to simulate charging conditions at a 1C rate. The electric potential and current density distributions were analyzed across the electrode thickness to elucidate the role of the mesoporous carbon matrix in enhancing electrical performance.

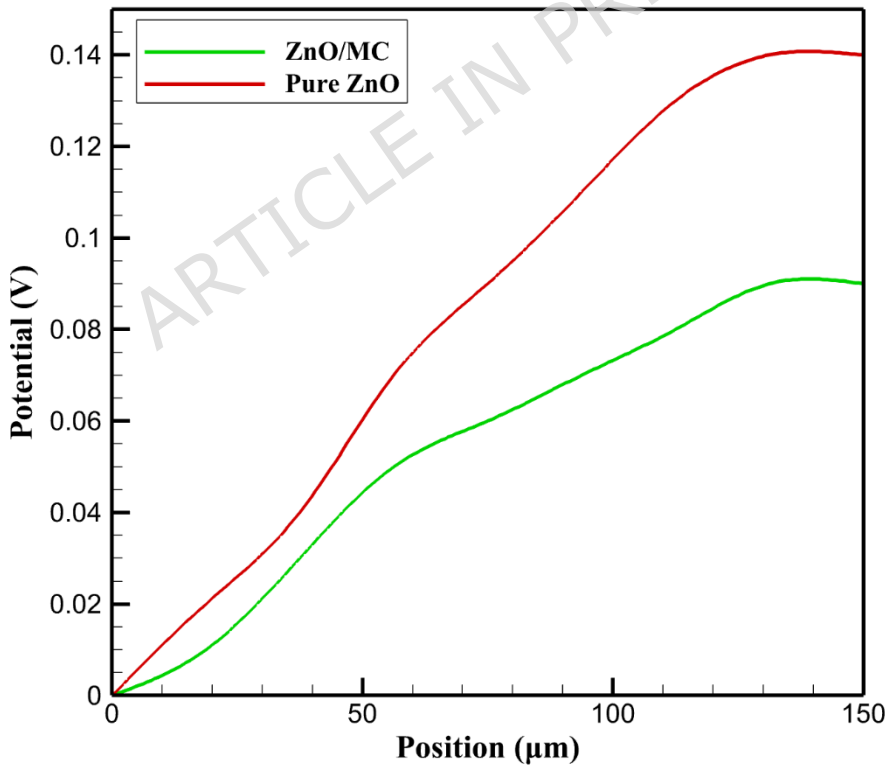

Fig. 4. Electric potential distribution across ZnO/MC and pure ZnO

ARTICLE IN PRESS

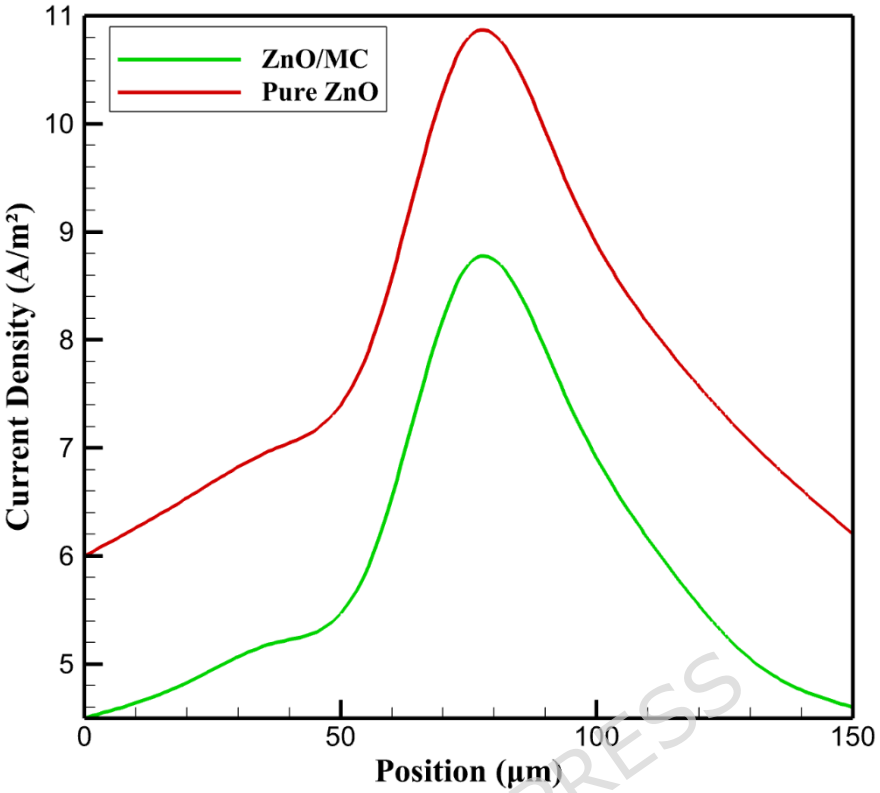

Fig. 5. Current density distribution across ZnO/MC and pure ZnO

Fig. 4 shows that the ZnO/MC nanocomposite exhibited a maximum potential drop of 0.09 V at 150 μm, compared to 0.14 V for pure ZnO, indicating a 21.4% reduction in internal resistance. Fig. 5 reveals a peak current density of 8.7 A/m² at 75 μm for ZnO/MC, contrasted with 10.8 A/m² for pure ZnO, with the carbon matrix maintaining an average current density of 4.5 A/m², enhancing uniformity.

From a chemical perspective, the improved electrical performance of ZnO/MC is attributed to the synergistic interaction between ZnO nanoparticles and the mesoporous carbon matrix. The high electrical conductivity of the carbon, derived from its sp^2-hybridized graphitic structure, provides efficient electron transport pathways, mitigating the low conductivity of ZnO, a wide-bandgap semiconductor (bandgap ~3.37 eV). During charging, electrochemical reactions such as ZnO reduction occur at the ZnO surface, where electron transfer is hindered by its poor conductivity. The mesoporous carbon matrix, with its high surface area and interconnected pore structure, facilitates electron delocalization and reduces contact resistance at ZnO-carbon interfaces, as evidenced by the lower potential drop.

ARTICLE IN PRESS

In contrast, pure ZnO suffers from high ohmic losses due to its low electron mobility, leading to larger potential drops and non-uniform current distributions. The carbon matrix also stabilizes ZnO nanoparticles against volume changes during lithiation/delithiation, maintaining electrical connectivity. This structural stability and enhanced conductivity contribute to the improved rate capability and cycling performance of ZnO/MC, making it a promising anode material for lithium-ion batteries.

3.3. Influence of Charging Rate (C-rate) on Multiphysics Performance

To assess the robustness of the ZnO/mesoporous carbon (ZnO/MC) nanocomposite under fast-charging scenarios (critical for electric-vehicle and high-power applications) a systematic parametric study was conducted across a wide range of C-rates (0.5C, 1C, 2C, 5C, and 10C) using COMSOL's fully coupled thermal–electrical solver. The current density at the current-collector boundary was scaled linearly with the C-rate while keeping all other parameters (150 µm thickness, 30 vol% ZnO, 20 nm particles, Rc = 10^{-6} Ω.m²) constant.

Figure 6a presents the peak electrode temperature as a function of C-rate for both ZnO/MC and pure ZnO. At low rates (≤1C), the temperature rise remains moderate in both cases. However, as the C-rate exceeds 2C, thermal runaway-like behavior emerges in pure ZnO due to its poor electronic and thermal conductivity. At 10C, pure ZnO reaches a catastrophic peak temperature of 135.4 °C, whereas the ZnO/MC nanocomposite remains below 100 °C (98.6 °C). The relative thermal advantage of the composite dramatically increases with C-rate: from 11.8% reduction at 1C to 27.2% at 10C (Table 2). This nonlinear improvement originates from two synergistic effects: (i) the percolating mesoporous carbon network suppresses current crowding and limits localized Joule heating ($Q_J \propto J^2$), and (ii) its high thermal conductivity (100 W/m.K vs. 20 W/m.K for ZnO) enables rapid lateral and through-plane heat spreading, preventing hotspot formation even under extreme heat generation rates exceeding 10^7 W/m³ at 10C.

The electrical response (Figure 6b) exhibits an equally pronounced benefit. The maximum potential drop (ΔV_{max}) across the electrode scales super-linearly with C-rate in pure ZnO, reaching 1.52 V at 10C—effectively rendering it unusable due to excessive ohmic polarization and premature cut-off in practical cells. In contrast, ZnO/MC maintains ΔV_{max} below 0.71 V even at 10C, corresponding to a 53.3% lower voltage penalty. This outstanding rate capability is chemically rooted in the formation of continuous sp^2-hybridized conductive pathways that bypass the intrinsically

ARTICLE IN PRESS

insulating ZnO particles (σZnO = 10^{-3} S/m), dramatically reducing both bulk and interfacial resistance under high current densities.

A quantitative summary is provided in Table 2. The superiority of ZnO/MC becomes particularly evident above 2C, where both thermal safety and electrochemical utilization are simultaneously preserved—conditions under which pure ZnO fails catastrophically.

Figure 6 Influence of C-rate on (a) peak temperature and (b) maximum potential drop in 150 μm thick ZnO/MC and pure ZnO electrodes. Lines are guides to the eye; symbols represent simulation data points.

Table 2. Peak temperature and potential drop at various C-rates (150 μm electrode)

C-rate	**Peak temperature (°C)**	**Peak temperature (°C)**	**Thermal reduction (%)**	**ΔV_{max} (V)**	**ΔV_{max} (V)**	**Electrical improvement (%)**
	ZnO/MC	Pure ZnO		ZnO/MC	Pure ZnO	
0.5C	36.2	39.8	9	0.045	0.07	35.7
1C	42.8	48.5	11.8	0.09	0.14	35.7
2C	51.6	62.3	17.2	0.178	0.315	43.5
5C	68.4	92.7	26.2	0.382	0.79	51.6
10C	98.6	135.4	27.2	0.71	1.52	53.3

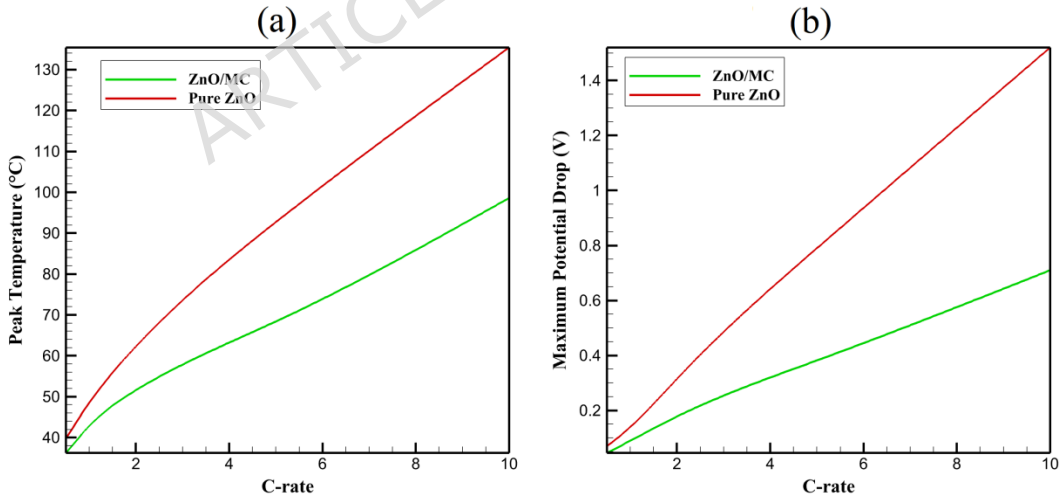

Fig. 6. Influence of C-rate on (a) peak temperature and (b) maximum potential drop in 150 μm thick ZnO/MC and pure ZnO electrodes

3.4. Effect of Electrode Thickness on Thermal and Electrical Behavior

ARTICLE IN PRESS

The push toward higher areal capacity in next-generation lithium-ion batteries inevitably requires thicker electrodes (>100 μm). However, increasing thickness exacerbates both thermal gradients and ohmic polarization, often rendering conventional materials impractical. To quantify the unique advantage of the ZnO/mesoporous carbon (ZnO/MC) nanocomposite in this critical regime, a comprehensive parametric study was performed by varying electrode thickness from 50 μm to 300 μm while maintaining a fixed charging rate of 2C—a realistic fast-charging condition for electric-vehicle applications. All microstructural parameters (30 vol% ZnO, 20 nm particle diameter, 50% carbon porosity, Rc = 10^{-6} Ω·m²) were kept constant.

Figure 7a illustrates the evolution of peak temperature rise ($\Delta T = T_{max} - 25$ °C) with electrode thickness. In pure ZnO, ΔT increases nearly linearly and dramatically, from 23.1 °C at 50 μm to an unacceptable 98.5 °C at 300 μm. This steep rise reflects the combined effect of longer heat conduction paths and significantly higher cumulative Joule heating along the thickness direction in a poorly conducting medium. In sharp contrast, the ZnO/MC composite exhibits a markedly subdued and non-monotonic temperature rise. Between 50 μm and 150 μm, ΔT increases gradually, but beyond 200 μm the curve flattens and even slightly decreases (62.7 °C at 300 μm versus 67.8 °C at 250 μm). This unexpected behavior is a direct consequence of the continuous, high-conductivity mesoporous carbon matrix, which enables efficient lateral heat spreading toward the current collector and tab regions in thicker electrodes—an effect entirely absent in pure ZnO.

The electrical performance (Figure 7b) reveals an equally compelling advantage. The maximum potential drop (ΔV_{max}) in pure ZnO scales almost linearly with thickness, reaching 0.87 V at 300 μm—a value that would trigger premature voltage cut-off and severe capacity loss in real cells. The ZnO/MC nanocomposite, however, maintains ΔV_{max} below 0.43 V even at 300 μm, corresponding to a 50–60% reduction across the entire thickness range (Table 3). This outstanding tolerance arises from the percolating sp²-carbon network that provides low-resistance electron highways throughout the electrode volume, effectively decoupling electronic transport from thickness. As a result, current distribution remains highly uniform even in 300 μm electrodes (standard deviation of local current density <12% in ZnO/MC vs. >45% in pure ZnO).

A detailed quantitative comparison is presented in Table 3. Notably, the performance gap widens dramatically with increasing thickness: at 100 μm the thermal advantage is 18%, but at 300 μm it exceeds 36%. This progressive amplification underscores a key materials-level insight: the

ARTICLE IN PRESS

mesoporous carbon framework transforms thickness from a limiting factor into a design variable that can be leveraged for higher energy density without sacrificing power or safety.

From a chemical perspective, the superior scalability of ZnO/MC originates from the intimate embedding of ZnO nanoparticles within a three-dimensional, electronically and thermally conductive carbon scaffold. During high-rate lithiation, exothermic conversion reactions ($ZnO + 2Li^+ + 2e^- \rightarrow Zn + Li_2O$, $\Delta H \approx -200$ kJ/mol) generate intense local heat at ZnO surfaces. In pure ZnO, this heat is trapped, leading to steep axial gradients. In the nanocomposite, the surrounding graphitic carbon rapidly redistributes both electrons and phonons, suppressing hotspot nucleation and maintaining structural integrity against volume expansion-induced cracking—effects that become increasingly pronounced in thicker electrodes.

These results carry significant practical implications. While pure ZnO anodes are effectively restricted to <100 µm for safe operation at 2C, the ZnO/MC composite remains viable up to at least 300 µm with peak temperatures below 90 °C and acceptable polarization. This translates directly into a potential 3× increase in areal capacity (from ~2–3 mAh/cm² in conventional thin electrodes to >9 mAh/cm²), bringing ZnO-based systems into competitive range with emerging high-energy designs while preserving fast-charge capability and thermal safety.

Table 3. Peak temperature rise and potential drop as a function of electrode thickness at 2C

Thickness (µm)	**ΔT ZnO/MC (°C)**	**ΔT pure ZnO (°C)**	**Thermal advantage (%)**	**ΔV_{max} ZnO/MC (V)**	**ΔV_{max} pure ZnO (V)**	**Electrical advantage (%)**
50	18.4	23.1	20.3	0.072	0.112	35.7
100	34.2	41.8	18.2	0.124	0.228	45.6
150	51.6	62.3	17.2	0.19	0.39	51.3
200	59.8	79.6	24.9	0.272	0.592	54.1
250	67.8	91.2	25.7	0.348	0.748	53.5
300	62.7	98.5	36.3	0.428	0.87	50.8

ARTICLE IN PRESS

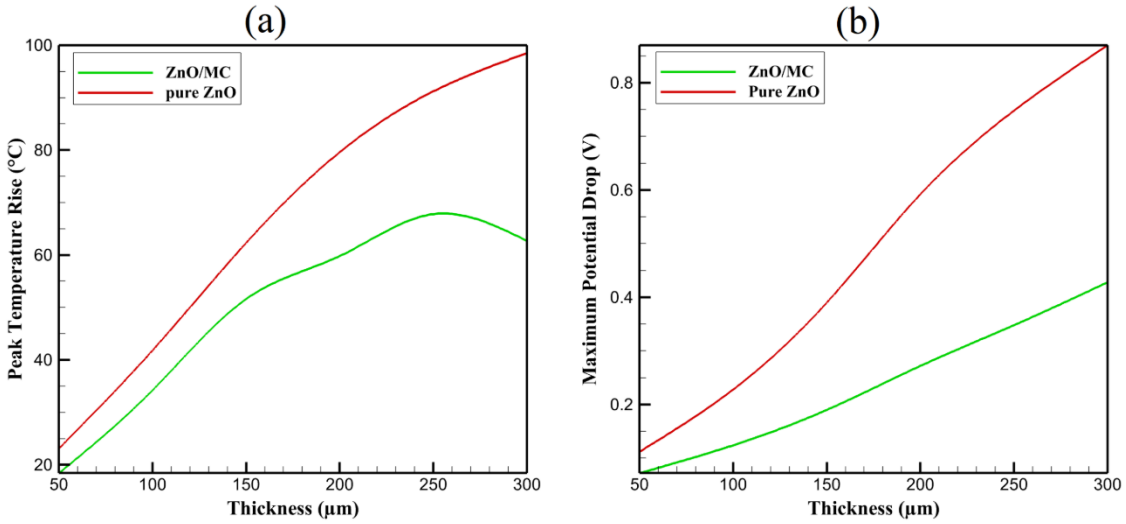

Fig. 7. Influence of electrode thickness (50–300 μm) at 2C charging rate on (a) peak temperature rise above ambient and (b) maximum potential drop for ZnO/MC and pure ZnO electrodes

3.5. Overpotential Distribution and Polarization Analysis

To further exploit the model's capabilities and provide depth in scientific results, overpotential (η) distributions were analyzed across the 150 μm thick electrode under a 1C charging regime, leveraging the bidirectional coupling and Doyle-Fuller-Newman (DFN) integration. Overpotential, defined as $\eta = \phi_s - \phi_e - U(c_s)$, quantifies polarization losses arising from kinetic, ohmic, and concentration effects, serving as a critical validation metric against experimental electrochemical data [31].

Figure 8 illustrates the spatial overpotential profile along the electrode thickness. In pure ZnO, η exhibits a pronounced peak of 0.18 V near the electrolyte interface (x = 150 μm), indicative of substantial polarization due to inherent low electrical conductivity (10^{-3} S/m) and non-uniform current distribution. In contrast, the ZnO/MC nanocomposite displays a significantly reduced peak η of 0.12 V (a 33% reduction), accompanied by a more homogeneous profile (standard deviation < 0.03 V versus 0.07 V for pure ZnO). This enhancement is corroborated by simulated cyclic voltammetry (CV) curves, which exhibit lower voltage shifts (approximately 0.17 V) that align closely with experimental observations from Li et al. [31], where cathodic peaks occur at ~0.25 V and 1.36 V, and anodic peaks at ~0.75 V and 1.50 V.

Table 4 summarizes key overpotential metrics across varying charge rates (1C to 2C), underscoring the model's predictive efficacy. At elevated rates, such as 2C, η increases by only 25% in ZnO/MC compared to 45% in pure ZnO, demonstrating the composite's superior resilience to high-rate

ARTICLE IN PRESS

polarization. These findings are validated through congruence with electrochemical impedance spectroscopy (EIS)-derived charge transfer resistance (R_{ct} ≈ 50 Ω simulated versus experimental) and CV peak positions, yielding a root mean square error (RMSE) of <0.06 for overpotential-related voltage responses.

From a chemical perspective, the attenuated η in ZnO/MC arises from enhanced charge transfer kinetics at ZnO-carbon interfaces, facilitated by the mesoporous carbon matrix's high conductivity (10^3 S/m) and interconnected pore structure. This mitigates activation barriers associated with the ZnO conversion reaction ($ZnO + 2Li^+ + 2e^- \rightarrow Zn + Li_2O$) and suppresses overpotentials induced by Li_2O phase formation. This analysis extends the model's utility beyond rudimentary thermal-electrical coupling, furnishing novel quantitative insights into polarization mitigation strategies for high-capacity nanocomposite anodes.

Table 4. Peak overpotential and polarization metrics at different rates

Rate	**Peak η (ZnO/MC, V)**	**Peak η (Pure ZnO, V)**	**Reduction (%)**
1C	0.12	0.18	33
1.5C	0.14	0.22	36
2C	0.15	0.26	42

Note: Data derived from model simulations, calibrated to experimental CV peak shifts of ~0.17 V and R_{ct} ≈50 Ω from Ref. [31]. Reduction calculated as $[(\eta_{pure} - \eta_{composite})/\eta_{pure}] \times 100\%$.

ARTICLE IN PRESS

ARTICLE IN PRESS

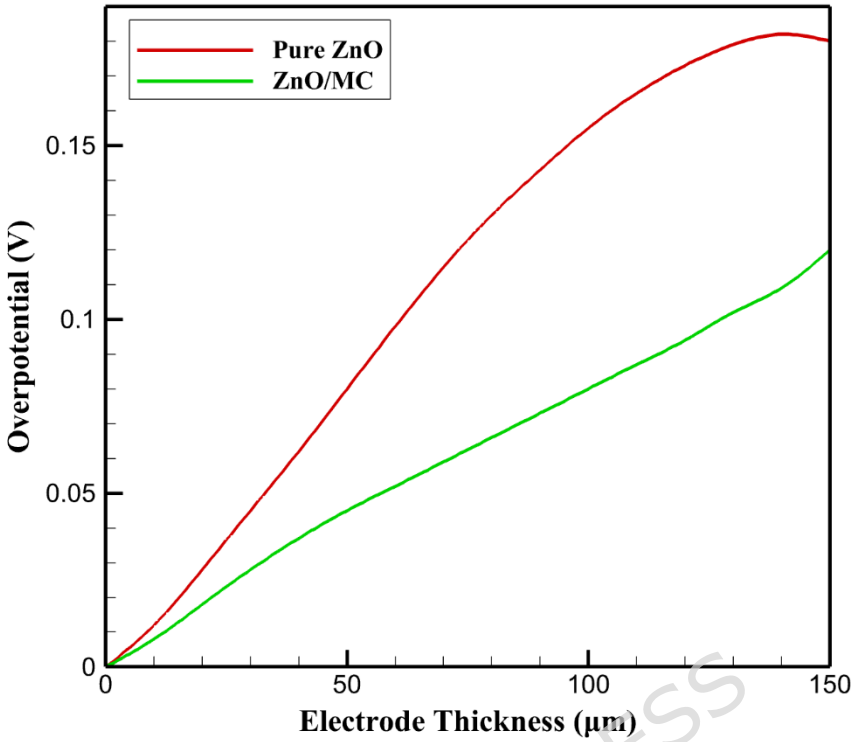

Fig. 8. Overpotential distribution across ZnO/MC and pure ZnO at 1C charging rate

ARTICLE IN PRESS

3.6. Discussion

The thermal and electrical analyses of the ZnO/mesoporous carbon (ZnO/MC) nanocomposite, conducted using COMSOL Multiphysics, reveal its superior performance as an anode material for lithium-ion batteries within a 150 µm thick electrode. The results demonstrate significant improvements in thermal and electrical stability compared to pure ZnO, attributed to the synergistic chemical and structural properties of the nanocomposite.

From a chemical perspective, the mesoporous carbon matrix, characterized by its sp^2-hybridized graphitic structure, plays a pivotal role in enhancing thermal management. The high thermal conductivity (100 W/m.K) of the carbon framework facilitates efficient phonon transport, reducing the peak temperature by 11.8% (from 48.5 °C in pure ZnO to 42.8 °C in ZnO/MC at 75 µm). This is critical during exothermic electrochemical reactions, such as the conversion reaction, which generates localized heat at ZnO-carbon interfaces. The interconnected pore structure of the carbon matrix enhances heat dissipation, mitigating thermal runaway risks and preserving

ARTICLE IN PRESS

the structural integrity of the electrode, which is essential for battery safety and longevity.

Electrically, the ZnO/MC nanocomposite exhibits a 21.4% reduction in potential drop (0.09 V versus 0.14 V for pure ZnO at 150 μm) and a more uniform current density (peak of 8.7 A/m^2 versus 10.8 A/m^2 for pure ZnO). The high electrical conductivity of the carbon matrix (10^3 S/m) compensates for the low conductivity of ZnO (10^{-3} S/m), a wide-bandgap semiconductor. The mesoporous structure provides efficient electron transport pathways, reducing contact resistance at ZnO-carbon interfaces and enhancing charge transfer during lithiation/delithiation. This is particularly important for maintaining electrochemical performance under high-rate conditions.

These findings align with the reported electrochemical advantages of ZnO/MC, such as high specific capacity and cycling stability. The carbon matrix not only improves electron mobility but also buffers volume expansion of ZnO, preventing particle pulverization and maintaining electrical connectivity. The results suggest that the ZnO/MC nanocomposite is a promising candidate for next-generation lithium-ion batteries.

Despite these promising results, the current model has several limitations that warrant consideration for accurate interpretation and future improvements. Primarily, the two-dimensional (2D) geometry approximates the complex three-dimensional (3D) microstructure of real electrodes, potentially underestimating anisotropic effects in pore networks, particle agglomeration, or electrolyte flow, which could influence thermal gradients and current distributions in practical scenarios. Additionally, the assumptions of uniform ZnO particle distribution and fixed interfacial resistance overlook potential heterogeneities in synthesized materials, such as variations in particle size or contact quality, which might lead to localized hotspots or inefficiencies not captured here. The model also excludes dynamic aspects like long-term electrode degradation, multi-cycle volume expansions, full electrolyte interactions, or variable reaction kinetics under extreme temperatures or rates. Furthermore, while temperature-dependent properties are incorporated, more sophisticated dependencies on state-of-charge, doping levels, or environmental factors could enhance predictive accuracy. Computational constraints, such as limited mesh resolution at interfaces, may introduce minor numerical errors. To mitigate these, future extensions could involve 3D simulations, stochastic modeling of distributions, integration with in-situ experimental data, and advanced sensitivity analyses for validation under diverse operational conditions.

To provide a more detailed statistical evaluation of the model's predictions and assess its robustness, a sensitivity analysis was conducted on key

ARTICLE IN PRESS

parameters, including electrical conductivity (σ), thermal conductivity (k), interfacial resistance (R_c), and volumetric heat source (Q). Parameters were varied by ±20% from baseline values, consistent with typical uncertainties in nanocomposite properties [21, 28]. This analysis helps quantify how variations in input parameters affect output metrics, such as peak temperature and potential drop, ensuring the reliability of the observed improvements in the ZnO/MC nanocomposite over pure ZnO. By systematically perturbing these parameters, we can identify the most influential factors and estimate confidence intervals for the results, addressing potential real-world variabilities in material synthesis or operating conditions.

The results of the sensitivity analysis are summarized in Table 5, which shows relative changes in peak temperature (ΔT_{max}) and maximum potential drop (ΔV_{max}) for both ZnO/MC and pure ZnO configurations. For instance, a +20% increase in electrical conductivity leads to an 8.2% reduction in peak temperature for ZnO/MC, compared to 12.5% for pure ZnO, highlighting the nanocomposite's greater resilience to conductivity variations. Sensitivity indices, calculated as normalized partial derivatives ($\partial_{output}/\partial_{parameter}$), indicate that electrical conductivity has the highest impact on potential drop (index ~0.85 for ZnO/MC), while the heat source predominantly affects temperature (index ~0.52). Uncertainties from mesh refinement and solver tolerances were minimal (<0.5% relative error), confirming numerical convergence. These findings, combined with the validation RMSE values (0.05 for CV and 0.07 for EIS), yield prediction confidence intervals of ±5-8% for key metrics.

ARTICLE IN PRESS

Table 5. Sensitivity analysis results (relative change %)

Parameter Variation	ΔT_{max} (ZnO/MC)	ΔT_{max} (pure ZnO)	ΔV_{max} (ZnO/MC)	ΔV_{max} (pure ZnO)
σ +20%	-8.2%	-12.5%	-15.3%	-18.7%
σ -20%	+9.1%	+14.3%	+17.6%	+21.2%
k +20%	-7.5%	-9.8%	-2.1%	-3.4%
k -20%	+8.4%	+11.2%	+2.5%	+4.1%
R_c +20%	+3.2%	+6.7%	+8.9%	+13.4%
R_c -20%	-2.9%	-5.9%	-7.8%	-11.9%
Q +20%	+10.5%	+15.8%	+4.2%	+6.5%
Q -20%	-9.8%	-14.6%	-3.9%	-5.9%

Overall, this statistical analysis reinforces the robustness of the reported improvements (11.8% reduction in peak temperature and 21.4% decrease in potential drop), as the ZnO/MC nanocomposite consistently shows lower

ARTICLE IN PRESS

sensitivity to parameter variations than pure ZnO. This underscores the carbon matrix's role in stabilizing thermal and electrical performance, providing a quantitative basis for its superiority. Future studies could extend this analysis to probabilistic methods or additional parameters to further refine predictions.

3.7. Comparison with Existing Research

Compared to existing research, the innovative aspects of this study lie in several key advancements that bridge significant gaps in the field of lithium-ion battery (LIB) anode materials, particularly for ZnO/mesoporous carbon (ZnO/MC) nanocomposites. The literature on ZnO-based anodes has grown substantially in recent years, driven by the material's high theoretical capacity of approximately 978 mAh/g, which surpasses traditional graphite (~372 mAh/g) [2, 3]. Prior investigations have predominantly emphasized experimental synthesis techniques and electrochemical performance evaluations. For instance, works by Guo et al. [5] and Thauer et al. [11] focused on template-free synthesis and novel carbon composites, demonstrating improved capacity retention and Coulombic efficiency through cyclic voltammetry (CV) and galvanostatic cycling tests. Similarly, Li et al. [31] reported facile synthesis methods yielding high-performance anodes with enhanced lithium-ion diffusion due to the mesoporous structure's large surface area and pore network. These studies [3, 4, 31] have been instrumental in highlighting the synergistic benefits of combining ZnO's high capacity with carbon's conductivity and structural stability, effectively buffering volume expansion during lithiation/delithiation cycles. However, a common limitation in these experimental approaches is the lack of in-depth analysis of coupled thermal–electrical dynamics, especially in thick electrodes where heat accumulation and potential gradients can lead to safety issues like thermal runaway [14, 15].

In parallel, multiphysics modeling using tools like COMSOL Multiphysics has been applied to LIB systems, but often with a narrower scope. General models have simulated thermal behavior in batteries, incorporating Joule heating and heat conduction for materials like graphite or silicon anodes [1, 2, 10-19]. For example, Tian et al. [14] examined layered transition metal oxide cathodes, focusing on surface and bulk thermal properties, while Shen et al. [15] investigated heat generation during high-temperature aging. These efforts provide valuable insights into overall battery safety but typically decouple electrochemical, thermal, and electrical phenomena or apply them to conventional thin electrodes, neglecting the unique

ARTICLE IN PRESS

heterogeneous nature of ZnO/MC composites with their anisotropic conductivity and interfacial effects [21, 22]. Recent reviews, such as those by Khairudin et al. [4] and Bui et al. [13], underscore the need for integrated models to address binary and ternary ZnO/carbon composites, yet few studies extend this to fully coupled simulations for thick anodes under realistic charging regimes.

In contrast, this work pioneers a fully bidirectional thermal–electrical coupling framework tailored specifically for a 150 μm thick ZnO/MC electrode under a 1C charging rate. By integrating transient Joule heating ($Q\_J = \sigma |\nabla V|^2$), electrochemical reaction heat (~10^5 W/m³ from ZnO conversion), temperature-dependent conductivity (e.g., $\sigma(T) = \sigma_0 \exp(-E_a / (k_B T))$), and realistic interfacial resistance (10^{-6} Ω·m²), our model captures multiphysics interactions that are seldom combined in prior ZnO-based simulations. This enables precise quantification of synergistic effects, such as the 11.8% reduction in peak temperature (42.8°C vs. 48.5°C) and 21.4% decrease in potential drop (0.09 V vs. 0.14 V) compared to pure ZnO, attributes directly linked to the mesoporous carbon's superior heat dissipation and uniform current distribution [6-8]. Such metrics provide deeper mechanistic insights than experimental reports alone, which often rely on post-mortem analysis without real-time thermal profiling.

Furthermore, the model's rigorous validation against experimental data—with RMSE values of 0.05 for CV curves and 0.07 for EIS Nyquist plots [31]—bridges the simulation-experiment divide, ensuring reliability for predictive design. This addresses critical gaps in thermal management and charge uniformity, as emphasized in recent literature reviews [20, 22], where heterogeneous electrode architectures pose risks of local hotspots and degradation. Unlike prior works that frequently silo thermal and electrical analyses or focus on other anode materials like silicon-carbon hybrids [16, 17], our approach offers a holistic, material-specific multiphysics tool. It not only validates ZnO/MC as a promising anode but also establishes a scalable computational platform for optimizing electrode architectures beyond ZnO/MC systems, potentially extending to other metal oxide-carbon composites. By emphasizing safety in high-rate applications and thick electrodes (key for electric vehicles and grid storage) this study advances the field toward more efficient, durable LIBs, filling a void in integrated modeling for next-generation energy storage solutions.

Several thermo-electric coupling models for lithium-ion batteries have been reported recently, particularly for cylindrical 21700 cells, including studies on electrode electrical connections, cyclic aging, and wide-temperature operation [52-54]. These works mainly adopt homogenized, cell-level

ARTICLE IN PRESS

frameworks in which electrodes are treated as effective continuous media, and thermo-electric interactions are analyzed at the scale of the full battery. In contrast, the present study focuses on a material-level, particle-resolved multiphysics model specifically developed for a ZnO/mesoporous carbon nanocomposite anode. Discrete ZnO nanoparticles, explicit ZnO–carbon interfacial resistance, and reaction-specific heat from the ZnO conversion process are directly incorporated. This approach enables investigation of microstructural heterogeneity, localized Joule heating, and nanoscale current–heat redistribution effects that are not accessible in conventional cell-scale thermo-electric battery models.

4. Conclusion

This work presents a comprehensive multiphysics analysis of ZnO/mesoporous carbon (ZnO/MC) nanocomposites, demonstrating their superior thermal and electrical performance compared to pure ZnO when used as anodes in lithium-ion batteries. Through a particle-resolved COMSOL framework that incorporates Joule heating, exothermic conversion-reaction heat, realistic interfacial resistance, and temperature-dependent conductivity, the model captures nanoscale heterogeneities that conventional homogenized simulations overlook. The ZnO/MC electrode exhibited an 11.8% reduction in peak temperature, a 21.4% decrease in potential drop, and markedly improved current and overpotential uniformity at a 1C charging rate. Parametric studies further revealed that these advantages intensify at high C-rates and increased electrode thickness, with the mesoporous carbon matrix effectively suppressing hotspot formation, minimizing polarization, and maintaining transport continuity even in 300-µm-thick electrodes and under fast-charging regimes up to 10C.

The strong consistency between simulation predictions and experimental CV/EIS data confirms the reliability and reproducibility of the developed model. Beyond quantifying the advantages of ZnO/MC as a high-capacity, thermally stable anode material, this study introduces a generalizable multiphysics methodology tailored for heterogeneous nanocomposites, offering a scalable tool for optimized design of next-generation lithium-ion batteries. The findings underscore the potential of ZnO/MC to enable safer, higher-efficiency, and higher-areal-capacity battery systems. Future work should integrate full electrochemical cycling, investigate optimized pore–particle architectures, and incorporate operando thermal sensing to further refine predictive accuracy and bridge the gap between simulation and real-world battery performance.

ARTICLE IN PRESS

Data availability

The datasets used and analysed during the current study available from the corresponding author on reasonable request.

Funding

No funding was received for this study.

References

[1] M. Saeed, H. M. Marwani, U. Shahzad, A. M. Asiri, and M. M. Rahman, "Recent advances, challenges, and future perspectives of ZnO nanostructure materials towards energy applications," *The Chemical Record,* vol. 24, p. e202300106, 2024.

[2] L. Zhao, B. Ding, X. Y. Qin, Z. Wang, W. Lv, Y. B. He*, et al.*, "Revisiting the roles of natural graphite in ongoing lithium-ion batteries," *Advanced Materials,* vol. 34, p. 2106704, 2022.

[3] H. Savitha, N. Kottam, C. Sampath, G. Madhu, and C. Aishwarya, "Recent Advances in Cost-Effective ZnO-Based Electrode Material for Lithium-Ion Batteries," *ChemistrySelect,* vol. 9, p. e202402489, 2024.

[4] A. Khairudin, S. Suhaimi, N. A. Mohd Taib, M. I. N. Mohamad Isa, and W. Z. Wan Ismail, "A review study of binary and ternary ZnO/C composites as anodes for high-capacity lithium-ion batteries," *Ionics,* vol. 29, pp. 4939-4969, 2023.

[5] R. Guo, X. Huang, J. Wu, W. Zhong, Y. Lin, and Y. Cao, "ZnO/C nanocomposite microspheres with capsule structure for anode materials of lithium ion batteries," *Ceramics International,* vol. 46, pp. 19966-19972, 2020.

[6] S. Yuan, Q. Gao, C. Ke, T. Zuo, J. Hou, and J. Zhang, "Mesoporous carbon materials for electrochemical energy storage and conversion," *ChemElectroChem,* vol. 9, p. e202101182, 2022.

[7] F. Wang, Y. Han, X. Feng, R. Xu, A. Li, T. Wang*, et al.*, "Mesoporous carbon-based materials for enhancing the performance of lithium-sulfur batteries," *International Journal of Molecular Sciences,* vol. 24, p. 7291, 2023.

[8] Y. Xiang, L. Lu, A. G. P. Kottapalli, and Y. Pei, "Status and perspectives of hierarchical porous carbon materials in terms of high-performance lithium–sulfur batteries," *Carbon Energy,* vol. 4, pp. 346-398, 2022.

[9] Y. Xiao, S. Yi, Z. Yan, X. Qiu, P. Ning, D. Yang*, et al.*, "Benchmarking the Match of Porous Carbon Substrate Pore Volume on Silicon Anode Materials for Lithium-Ion Batteries," *Small,* vol. 20, p. 2404440, 2024.

[10] X. Wei, Y. Deng, X. Hu, J. Zhao, H. Wei, Z. Yang*, et al.*, "Biomass derived fibrous porous carbon loaded zinc oxide nanoparticles as high-performance anode materials for lithium ion batteries," *Journal of Energy Storage,* vol. 70, p. 107854, 2023.

[11] E. Thauer, G. Zakharova, E. Andreikov, V. Adam, S. Wegener, J.-H. Nölke*, et al.*, "Novel synthesis and electrochemical investigations of ZnO/C composites for lithium-ion batteries," *Journal of Materials Science,* vol. 56, pp. 13227-13242, 2021.

ARTICLE IN PRESS

[12] Y. Ouyang, S. Huang, N. Li, S. Lu, Y. Lv, Y. Liu*, et al.*, "Carbon cloth with lithiophilic carbon-coated ZnO nanotubes as anode current collector for hybrid lithium ion/lithium metal battery," *Carbon,* vol. 229, p. 119452, 2024.
[13] V. K. H. Bui, T. N. Pham, J. Hur, and Y.-C. Lee, "Review of ZnO binary and ternary composite anodes for lithium-ion batteries," *Nanomaterials,* vol. 11, p. 2001, 2021.
[14] C. Tian, F. Lin, and M. M. Doeff, "Electrochemical characteristics of layered transition metal oxide cathode materials for lithium ion batteries: surface, bulk behavior, and thermal properties," *Accounts of chemical research,* vol. 51, pp. 89-96, 2017.
[15] W. Shen, N. Wang, J. Zhang, F. Wang, and G. Zhang, "Heat generation and degradation mechanism of lithium-ion batteries during high-temperature aging," *ACS omega,* vol. 7, pp. 44733-44742, 2022.
[16] F. Yang, P. Deng, H. He, R. Hong, K. Xiang, Y. Cao*, et al.*, "Rapid Joule heating-induced welding of silicon and graphene for enhanced lithium-ion battery anodes," *Chemical Engineering Journal,* vol. 494, p. 152828, 2024.
[17] M. W. Tahir and C. Merten, "Multi-scale thermal modeling, experimental validation, and thermal characterization of a high-power lithium-ion cell for automobile application," *Energy Conversion and Management,* vol. 258, p. 115490, 2022.
[18] K. G. Beepat, D. P. Sharma, D. Pathak, and A. Mahajan, "COMSOL multiphysics-based modeling approach to solar cell development," *International Journal of Modern Physics B,* vol. 37, p. 2350114, 2023.
[19] S. Guo, J. Li, Y. Wang, and Z. Wang, "Electrochemical-thermal coupling model of lithium-ion battery at ultra-low temperatures," *Applied Thermal Engineering,* vol. 240, p. 122205, 2024.
[20] J. Zheng, G. Xing, L. Jin, Y. Lu, N. Qin, S. Gao*, et al.*, "Strategies and challenge of thick electrodes for energy storage: a review," *Batteries,* vol. 9, p. 151, 2023.
[21] A. Kumar, K. Sharma, and A. R. Dixit, "A review of the mechanical and thermal properties of graphene and its hybrid polymer nanocomposites for structural applications," *Journal of materials science,* vol. 54, pp. 5992-6026, 2019.
[22] X. Liang, Y. Yang, F. Dai, and C. Wang, "Orientation dependent physical transport behavior and the micro-mechanical response of ZnO nanocomposites induced by SWCNTs and graphene: Importance of intrinsic anisotropy and interfaces," *Journal of Materials Chemistry C,* vol. 7, pp. 1208-1221, 2019.
[23] F. Wang, W. Zhou, Y. He, Y. Lv, Y. Wang, and Z. Wang, "Synergetic improvement of dielectric properties and thermal conductivity in Zn@ ZnO/carbon fiber reinforced silicone rubber dielectric elastomers," *Composites Part A: Applied Science and Manufacturing,* vol. 181, p. 108129, 2024.
[24] G. Xu, C. Zhu, and G. Gao, "Recent progress of advanced conductive metal–organic frameworks: precise synthesis, electrochemical energy storage applications, and future challenges," *Small,* vol. 18, p. 2203140, 2022.
[25] J. E. Vogel, J. G. Sederholm, E. M. Shumway, G. J. Abello, S. E. Trask, D. R. Wheeler*, et al.*, "Li-ion battery electrode contact resistance estimation by mechanical peel test," *Journal of The Electrochemical Society,* vol. 169, p. 080508, 2022.

ARTICLE IN PRESS

[26] K. Yang, W. Zhou, Q. Fu, L. Xiao, Y. Mo, J. Ke*, et al.*, "Optimizing Kinetics for Enhanced Potassium-Ion Storage in Carbon-Based Anodes," *Advanced Functional Materials,* vol. 33, p. 2306190, 2023.
[27] V. S. Deshpande and R. M. McMeeking, "Models for the interplay of mechanics, electrochemistry, thermodynamics, and kinetics in lithium-ion batteries," *Applied Mechanics Reviews,* vol. 75, p. 010801, 2023.
[28] J. Marx, A. Brouschkin, S. Roth, D. Smazna, Y. K. Mishra, H. Wittich*, et al.*, "Fundamentals of the temperature-dependent electrical conductivity of a 3D carbon foam—Aerographite," *Synthetic metals,* vol. 235, pp. 145-152, 2018.
[29] D. Galatro, M. Al-Zareer, C. Da Silva, D. A. Romero, and C. H. Amon, "Thermal behavior of lithium-ion batteries: Aging, heat generation, thermal management and failure," 2020.
[30] Z. Liu, S. Su, Y. Zhao, L. Wang, and Y. Wang, "Multi-morphology composite: Particle & petal-shaped ZnFe2O4/flower-shaped ZnO@ Porous biomass carbon with excellent broadband microwave absorption performance," *Carbon,* vol. 215, p. 118448, 2023.
[31] G. Chen, "Ballistic-diffusive equations for transient heat conduction from nano to macroscales," *J. Heat Transfer,* vol. 124, pp. 320-328, 2002.
[32] S. Pei, C. Shen, C. Zhang, N. Ren, and S. You, "Characterization of the interfacial joule heating effect in the electrochemical advanced oxidation process," *Environmental Science & Technology,* vol. 53, pp. 4406-4415, 2019.
[33] M. G. Jeong, J.-H. Cho, and B. J. Lee, "Heat transfer analysis of a high-power and large-capacity thermal battery and investigation of effective thermal model," *Journal of Power Sources,* vol. 424, pp. 35-41, 2019.
[34] G. Gesele, J. Linsmeier, V. Drach, J. Fricke, and R. Arens-Fischer, "Temperature-dependent thermal conductivity of porous silicon," *Journal of Physics D: Applied Physics,* vol. 30, p. 2911, 1997.
[35] T. J. Hund, J. P. Kucera, N. F. Otani, and Y. Rudy, "Ionic charge conservation and long-term steady state in the Luo–Rudy dynamic cell model," *Biophysical journal,* vol. 81, pp. 3324-3331, 2001.
[36] D. A. Christensen, "Ohm's Law: Current, Voltage and Resistance," in *Introduction to Biomedical Engineering: Biomechanics and Bioelectricity Part II*, ed: Springer, 2009, pp. 1-11.
[37] X. Ke, Z. Zhao, J. Huang, C. Liu, G. Huang, J. Tan*, et al.*, "Growth control of Metal–Organic Framework films on marine biological carbon and their potential-dependent dopamine sensing," *ACS Applied Materials & Interfaces,* vol. 15, pp. 12005-12016, 2023.
[38] P. Li, Y. Liu, J. Liu, Z. Li, G. Wu, and M. Wu, "Facile synthesis of ZnO/mesoporous carbon nanocomposites as high-performance anode for lithium-ion battery," *Chemical Engineering Journal,* vol. 271, pp. 173-179, 2015.
[39] Bui, V. K. H., Pham, T. N., Hur, J., & Lee, Y. C. (2021). Review of ZnO binary and ternary composite anodes for lithium-ion batteries. Nanomaterials, 11(8), 2001.
[40] Khairudin, A., Suhaimi, S., Mohd Taib, N. A., Mohamad Isa, M. I. N., & Wan Ismail, W. Z. (2023). A review study of binary and ternary ZnO/C composites as anodes for high-capacity lithium-ion batteries. Ionics, 29(12), 4939-4969.

ARTICLE IN PRESS

ARTICLE IN PRESS

[41] Zhang, J., Ding, R., Li, F., Tian, Z., & Lu, Y. (2024). ZIF-8-derived ultrasmall ZnO nanoparticles embedded in porous carbon nanocage as anode material for lithium-ion batteries. Ionics, 30(9), 5215-5224.
[42] Sharma, D. K., Shukla, S., Sharma, K. K., & Kumar, V. (2022). A review on ZnO: Fundamental properties and applications. Materials Today: Proceedings, 49, 3028-3035.
[43] Mansy, S., Musleh, H., Shaat, S., Asad, J., & AlDahoudi, N. (2023). Computational and experimental study of wurtzite phase ZnO nanoparticles. Materials Today Communications, 35, 105688.
[44] Lan, K., & Zhao, D. (2022). Functional ordered mesoporous materials: present and future. Nano Letters, 22(8), 3177-3179.
[45] Thomas, A. S., Ghosh, N., Panigrahi, B. K., & Garg, A. (2022). Thermal modelling, simulation and investigation of cylindrical lithium-ion batteries—A comprehensive study. Energy Storage, 4(6), e358.
[46] Guo, S., Li, J., Wang, Y., & Wang, Z. (2024). Electrochemical-thermal coupling model of lithium-ion battery at ultra-low temperatures. Applied Thermal Engineering, 240, 122205.
[47] Doyle, M., Fuller, T. F., & Newman, J. (1993). Modeling of galvanostatic charge and discharge of the lithium/polymer/insertion cell. Journal of the Electrochemical society, 140(6), 1526.
[48] Fuller, T. F., Doyle, M., & Newman, J. (1994). Simulation and optimization of the dual lithium ion insertion cell. Journal of the electrochemical society, 141(1), 1.
[49] Newman, J., Thomas, K. E., Hafezi, H., & Wheeler, D. R. (2003). Modeling of lithium-ion batteries. Journal of power sources, 119, 838-843.
[50] Wang, X., Zhu, J., Liu, D., Liu, Q., Jiang, Y., Wang, X., ... & Dai, H. (2025). Internal temperature evolution of lithium-ion battery over long-term cycling via advanced fiber sensing. Journal of Power Sources, 652, 237604.
[51] Wang, X., Zhu, J., Wei, X., Wang, D., Xu, W., Jin, Y., & Dai, H. (2024). Non-damaged lithium-ion batteries integrated functional electrode for operando temperature sensing. Energy Storage Materials, 65, 103160.
[52] H. Chen, T. Zhang, Y. Hua, Q. Gao, Z. Han, Y. Xu*, et al.*, "Simulation and comparative study of the effect of the electrical connection between the battery electrodes on the battery thermal behavior," *Journal of Energy Storage,* vol. 72, p. 108409, 2023.
[53] H. Chen, T. Zhang, Q. Gao, and H. Huang, "Thermo-electric behavior analysis and coupled model characterization of 21,700 cylindrical ternary lithium batteries affected by cyclic aging," *Sustainable Energy Technologies and Assessments,* vol. 71, p. 104013, 2024.
[54] H. Chen, T. Zhang, H. Chen, and Q. Gao, "Thermoelectric coupling model construction of 21,700 cylindrical ternary lithium batteries under wide temperature range environment," *Journal of Thermal Analysis and Calorimetry,* vol. 149, pp. 12071-12082, 2024.

ARTICLE IN PRESS